Available online at www.sciencedirect.com
SCIENCE DIRECT
Trans. Nonferrous Met. Soc. China 17(2007) 874−879
Transactions of Nonferrous Metals Society of China
www.csu.edu.cn/ysxb/

Preparation and properties of $Ce_{0.8}Ca_{0.2}O_{1.8}$ anode material by glycine-nitrate process

LIU Rong-hui(刘荣辉)[1, 2], MA Wen-hui(马文会)[1, 2],
WANG Hua(王 华)[1], YANG Bin(杨 斌)[1, 2], DAI Yong-nian(戴永年)[1, 2]

1. Faculty of Materials and Metallurgical Engineering, Kunming University of Science and Technology, Kunming 650093, China;
2. National Engineering Laboratory of Vacuum Metallurgy, Kunming University of Science and Technology, Kunming 650093, China

Received 8 October 2006; accepted 28 May 2007

Abstract: $Ce_{0.8}Ca_{0.2}O_{1.8}$ (CDC82) anode material was prepared by glycine-nitrate process(GNP). Thermogravimetric(TG) analysis and differential scanning calorimetric(DSC) methods were adopted to characterize the reaction process of CDC82 material. X-ray diffractometry(XRD), scanning electron microcopy(SEM), direct current four probe (four-probe DC) and temperature process reduce(TPR) techniques were adopted to characterize the properties of CDC82 material. After the precursor was sintered at 750 ℃ for 4 h, CDC82 material with pure-fluorite structure and nanometer size was obtained. The total conductivity of CDC82 changes little with temperature in air at 50−850 ℃, and the maximum value is 0.04 S/cm at 750 ℃. The total conductivity wholly becomes larger when the atmosphere changes from air to hydrogen, which greatly increases with increasing temperature and reaches the maximum value of 1.09 S/cm at 850 ℃. Some impurities such as CeMg and La_2O_3 exist after the mixture of CDC82 anode and $La_{1-x}Sr_xGa_{1-y}Mg_yO_{3-\delta}$ (LSGM) electrolyte material is sintered at 1 200 ℃ for 15 h. The CDC82 material as anode material has excellent catalytic property for hydrogen and methane.

Key words: $Ce_{0.8}Ca_{0.2}O_{1.8}$; anode material; glycine-nitrate process; conductivity; chemical compatibility; catalytic property

1 Introduction

Anode material is one of the key components of solid oxide fuel cell (SOFC). The precious metals such as platinum and silver were used as anode material at first, but they have few applications now for some reasons such as high price and evaporation of silver [1−3]. Then, the cheaper nickel was applied to be anode material, but the porous nickel anode becomes dense and the cell's performance deteriorates after a long operation at high temperature. Now, the nickel-electrolyte composite material is often used as anode. Many problems such as the serious agglomeration of anode, carbon deposition at anode when using fuel containing carbon and the poor tolerance of sulfur still exist [1, 4]. Furthermore, the total conductivity of anode decreases for the relatively low conductivity of electrolyte (such as YSZ and LSGM) materials, and the catalytic property of composite anode becomes poor because the above electrolyte materials don't offer catalytic properties. So, the design and synthesis of novel anode materials are necessary. These novel anode materials must have high mixed (ionic and electronic) conductivity and excellent catalytic property at low and intermediate (600−800 ℃) temperatures.

The CeO_2-based materials as electrolyte of the low temperature SOFC were studied by ZHA et al [5] and XIA et al [6]. Oxygen vacancies emerge when CeO_2 is doped by Sm^{3+} and Gd^{3+} and the conductivity greatly increases [7−9]. The three-phase boundary for the electrochemical reaction at anode increases when CeO_2-based electrolyte material is added to anode material. There are the following good results through the above operation. Ce^{4+} is reduced to Ce^{3+} in reducing atmosphere and the total conductivity increases on a large scale, which neutralizes the ohmic loss for the adulteration of the traditional electrolyte. The CeO_2-based materials have excellent catalytic properties and are often applied in the water-vapor reforming and

Foundation item: Projects(50204007; 50574046) supported by the National Natural Science Foundation of China; Project(2005PY01-33) supported by the Natural Foundation of Yunnan Province, China
Corresponding author: MA Wen-hui; Tel/Fax: +86-871-5161583; E-mail: mwhui@kmust.edu.cn

direct degradation of hydrocarbon industry [10−11]. So, the CeO_2-based anode materials have a good promising prospect in SOFC using hydrocarbon as fuel.

In this study, the $Ce_{0.8}Ca_{0.2}O_{1.8}$ (CDC82) material was synthesized by glycine-nitrate process (GNP), the conductivity of this material at different temperatures in oxidizing and reducing atmospheres, the catalytic properties for hydrogen and methane, and the chemical compatibility with LSGM electrolyte material were studied systematically.

2 Experimental

2.1 Preparation of CDC82 material and phase characterization

Raw materials including $Ce(NO_3)_4{\cdot}6H_2O$ (99.99%) and Ca $(NO_3)_2$ (99.99%). $Ce(NO_3)_4{\cdot}6H_2O$ and $Ca(NO_3)_2$ with a molar ratio of 8:2 were resolved into distilled water. Glycine (the molar ratio of glycine to metal was 2:1) was then added to the above solution. The solution was subsequently heated to form gel and strenuously combusted at about 250 ℃, and then the precursor for CDC82 material was obtained. It is difficult to capture the precursor powder because the powder will spray strenuously in the combustion process. A stainless steel mesh was put onto the beaker. By doing this, the exhaust gas can get out from the beaker and the precursor was stayed in the reactor. Thermogravimetric(TG) analysis and differential scanning calorimetric(DSC) methods were adopted to confirm the synthesis temperature at 25−1 200 ℃. The precursor for CDC82 material was sintered at 750 ℃ for 4 h to remove residual carbon and promote crystallization of the fluorite phase. The crystal structure of the CDC82 powder was examined at room temperature with Bruker D8 diffractometer. The size of the sintering material was observed by scanning electron microcopy (SEM, Philips XL30ESEM).

2.2 Total conductivity measurements

The calcined precursors for CDC82 material were isostatically pressed into pellets (*d*13 mm×3 mm) at load of 120 MPa. The CDC82 pellet was sintered at 1 300 ℃ for 5 h. After the treatment of the sintering sample, Ag paste was coated on the pellet and sintered at 850 ℃ for 1 h to reduce the organism, and then Ag electrode was prepared. Ag wire was attached to the Ag electrode. The four-probe direct current technique was adopted to measure the total conductivity (ionic and electronic) of the CDC82 pellets at 250−850 ℃. The stationary current was supplied by the current source (East Changing Technologies, Inc., Beijing) that can change from 2 nA to 2 A.

2.3 Compatibility of CDC82 and LSGM materials

The anode was connected with the electrolyte in SOFC. They shouldn't react with each other in the fabrication and operation process of SOFC. That is to say, they should have good chemical compatibility. CDC82 material has naturally good chemical compatibility with CeO_2-based electrolyte material, and the chemical compatibility between CDC82 and LSGM electrolyte material was characterized in this experiment.

To investigate the chemical compatibility between LSGM and CDC82 materials, LSGM and CDC82 materials were mixed with the mass ratio of 1:1, ground homogeneously with alcohol in the agate mortar, dried in the vacuum drying chamber, and sintered at 1 200 ℃ in air for 15 h in the muffle furnace. XRD was used to determine whether there is chemical reaction between LSGM and CDC82. In general, the operation temperature of intermediate temperature SOFC is about 800 ℃. By considering higher temperature necessary for SOFC fabrication and resulted from non-homogeneous heating during operation of cell, the temperature of 1 200 ℃ was taken as criterion.

2.4 Catalytic property

Temperature process reducing(TPR) experiments of CDC82 material were performed in the TPR equipment (Quantachrome, Win v 1.50). The carrier gas was pure hydrogen and its flow rate was 75 mL/min, the mass of CDC82 material was 0.1 g, and the experimental temperature changed from room temperature to 790 ℃ at a rate of 5 ℃/min.

The experiment of catalytic property for methane was operated in a laboratory-made fixed bed. The experimental gas consisted of a mixture of 90%CH_4 (molar fraction) and 10%Ar (molar fraction), its rate was 20 mL/min, the mass of the catalysis was 2 g, and the operation temperature was 850 ℃. The tail gas composition was checked by gas chromatography (GC112A, Analytical Instrument Factory in Shanghai). The content of water could not be checked by this method.

3 Results and discussion

3.1 TG- DSC analysis

Fig.1 shows the TG-DSC curves of the precursors of CDC82 materials. There is an endothermic peak at about 100 ℃ in the DSC curve, and an initial mass loss of 5.87% between 100 ℃ and 320 ℃, corresponding to the loss of the bound water. There is an exothermal peak at about 320 ℃, the second mass loss of 4.69% between 320 ℃ and 567 ℃, corresponding to the decomposition of the residual nitrate and the elimination of the incomplete glicine combustion. The mass of the material

decreases more quickly from about 567 ℃, corresponding to the release of crystal oxygen resulted from the replacement of Ce^{4+} by Ca^{2+}. No obvious endothermic or exothermal peaks exist on the DSC curve at about 567 ℃. The last exothermal peak emerges at about 829 ℃, but the changing rate of the thermal mass loss becomes smooth above this temperature. Maybe, this exothermal peak results from the transition of the crystal structure. Theoretically, the CDC82 material with fluorite can be formed above 566 ℃.

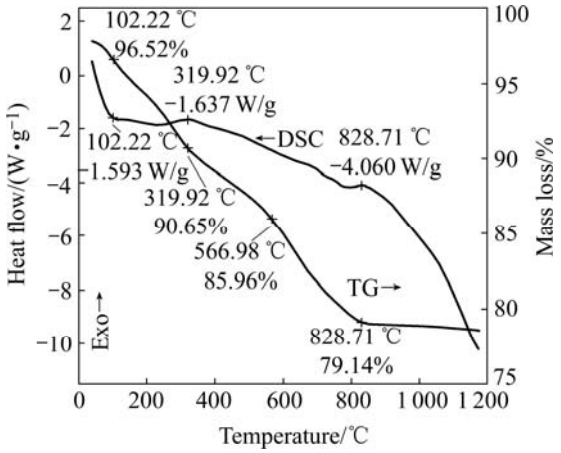

Fig.1 TG and DSC curves of precursors of CDC82 material

3.2 XRD and SEM of prepared materials

Fig.2 shows the XRD pattern of CDC82 powder sintered at 750 ℃ for 4 h. Pure fluorite phase exists after the predecessor is sintered at 750 ℃ for 4 h, which indicates that Ca^{2+} replaces Ce^{4+} well. The result of XRD accords with that of thermal analysis (TG-DSC). According to Fig.2, the diffraction peaks of CDC82 powder are very sharp, displaying that the crystal crystalline grains grow well.

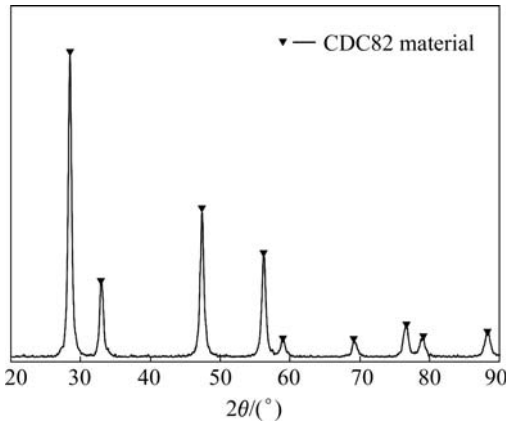

Fig.2 XRD pattern of precursor of CDC82 powder sintered at 750 ℃ for 4 h

Fig.3 shows the SEM images of the CDC82 anode material sintered at 750 ℃ for 4 h. According to the images, the crystalline grains agglomerate and form large size particles. But the diameters of most particles are below 30 μm. CDC82 powder with nanometer size can be obtained after grinding. The small size particles are very active, which is beneficial to decreasing the fabrication temperature of the anode film and improving the catalytic properties.

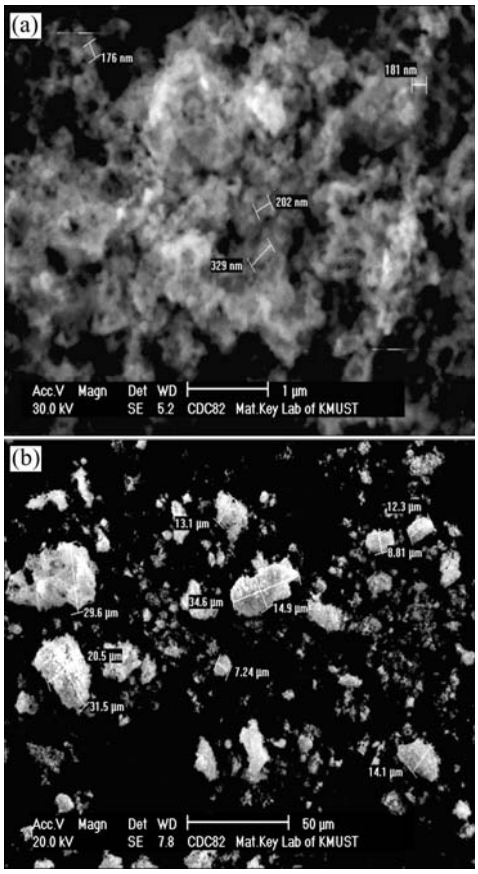

Fig.3 SEM images of CDC82 material sintered at 750 ℃ for 4 h: (a) Higher magnification; (b) Lower magnification

Fig.4 shows SEM images of the CDC82 anode pellet sintered at 1 300 ℃ for 5 h. According to the images, the crystalline grains with roll shape offer nanometer size. The grains are closely packed and no voids are observed between the crystalline grains. This dense pellet can efficiently prevent fuel in anode chamber and oxygen in cathode chamber from permeating from one side to another side and can enlarge cell efficiency when it is used as the electrolyte layer of SOFC. It is verified that the CDC82 material sintered at 750 ℃ is very active.

3.3 Conductivity of samples

Fig.5 shows the total conductivity of CDC82 in air and pure hydrogen, which was measured by four-probe direct current method at different temperatures. The oxygen vacancies exist when Ce^{4+} is replaced by Ca^{2+} in air, and the material has low ionic conductivity. The ionic conductivity changes little at 250−850 ℃, and reaches

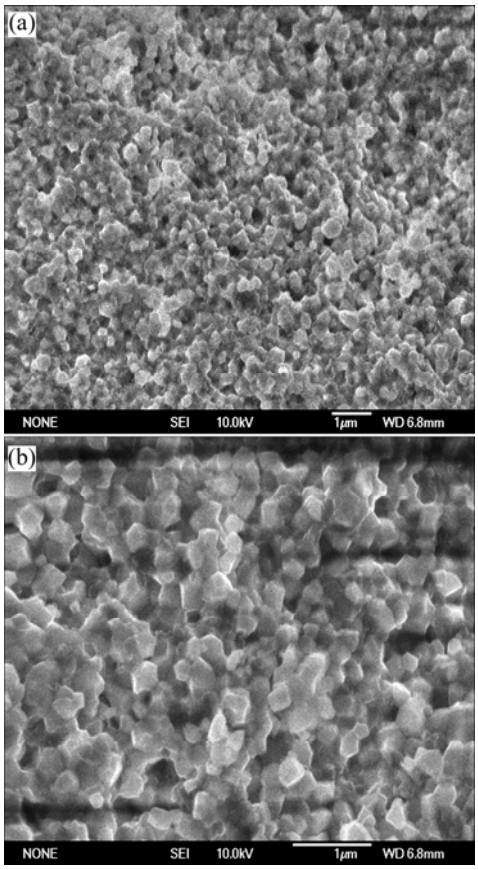

Fig.4 SEM images of CDC82 pellet sintered at 1 300 ℃ for 5 h: (a) Lower magnification; (b) Higher magnification

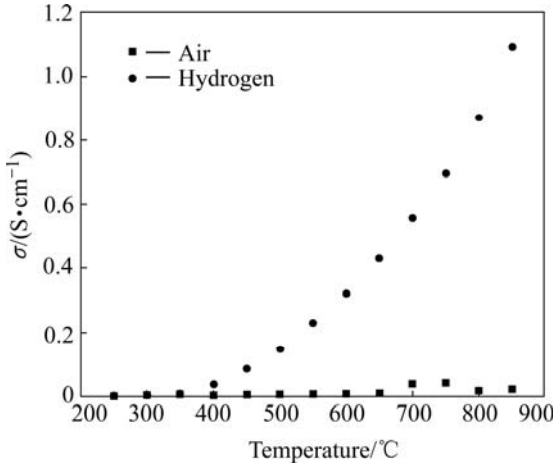

Fig.5 Conductivity of CDC82 material at different temperatures in different atmospheres

the maximum value of 0.04 S/cm at 750 ℃.

Ce^{4+} is reduced to Ce^{3+} when the experimental atmosphere changes from air to hydrogen. In order to analyze the correlation between conductivity and atmosphere, the thermodynamic analysis of the reaction of CDC82 and H_2 is necessary. For the shortage of thermodynamic data of CDC82 and the similarity between CDC82 and CeO_2, the thermodynamic analysis of CeO_2 and H_2 was carried out by HSC thermodynamic software that can response that of CDC82 and H_2 to a certain extent[12−13].

Fig.6 shows the equilibrium diagram with the main species using CeO_2 and H_2 as starting materials at different temperatures. From Fig.6, CeO_2 can be reduced to $CeO_{1.83}$ and $CeO_{1.72}$ at low temperatures, and more and more Ce^{4+} changes to Ce^{3+} with temperature increasing. So, the electrical type changes from ionic to ionic-electronic mixed one when the experimental atmosphere changes from air to hydrogen, and the total conductivity increases.

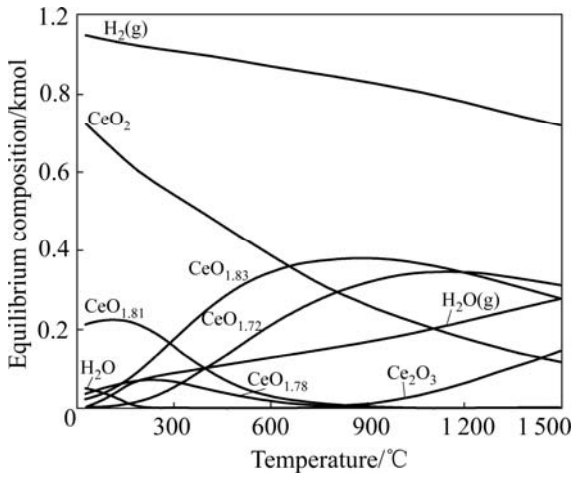

Fig.6 Equilibrium diagram of reaction of CeO_2 and H_2 at various temperatures

According to Fig.6, only a small amount of Ce^{4+} are reduced in hydrogen below 400 ℃. Correspondingly, the total conductivity changes little under this conditions. More and more Ce^{4+} ions are reduced to Ce^{3+} above 400 ℃ and more Ce^{4+}/Ce^{3+} small polarons form. Furthermore, the small polarons have high energy and can move more quickly at higher temperatures. So, the total conductivity increases more rapidly above 400 ℃, for example, it reaches 1.09 S/cm at 850 ℃.

3.4 Chemical compatibility between CDC82 and LSGM materials

Fig.7 shows the XRD patterns of the mixed powders of LSGM and CDC82 materials sintered at 1 200 ℃ in air for 15 h. According to Fig.7, the impurities such as La_2O_3 and CeMg emerge during the heating process. This result shows that there is a chemical reaction between LSGM and CDC82 materials. The conventional (coating and screen-printing) techniques aren't suitable for the fabrication of LSGM-based CDC82 anode film. Maybe, the application of some special techniques (such as plasma spray [14] and pulsed laser deposition [15]) without sintering process at high temperature or the

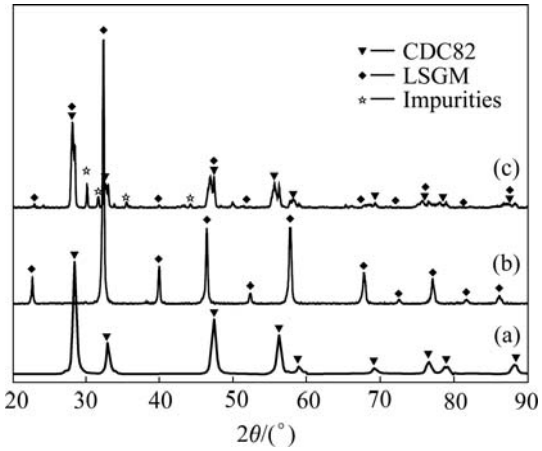

Fig.7 XRD patterns of CDC82(a), LSGM(b) and mixture of them(c) sintered at 1 200 ℃ for 15 h

introduction of an interlayer between CDC82 and LSGM [16] can resolve the above problem.

In the experiments, the CeMg impurity emerges in the sintering process of LSGM-$Ce_{1-x}Ca_xO_{2-\delta}$ and LSGM-$Ce_{1-x}Gd_xO_{2-\delta}$. It is assumed that CeMg results from the diffusion of Mg and the reaction between Mg and CeO_2-based materials. In order to find the reason for this phenomenon, the equilibrium diagram of CeO_2-Mg is drawn by HSC thermodynamic software (Fig.8). According to Fig.8, CeMg alloy emerges at low temperature, and Mg element permeates into CeO_2-based materials continuously. So, the perovskite structure of LSGM is damaged and the impurities such as La_2O_3 emerge.

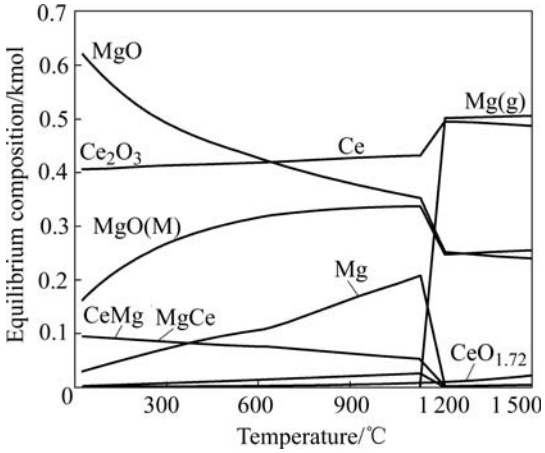

Fig.8 Equilibrium diagram of reaction of CeO_2 and Mg at various temperatures

3.5 Catalytic properties

TPR profile of CDC82 material is shown in Fig.9. It can be noticed that the reduction of the CDC82 material takes place in two stages. Maximal peaks locate at 470 ℃ and 600 ℃. The first peak is involved in the reduction of the surface sites, while the second peak in bulk sites. Compared with the two reduction peaks (380 ℃ and 800 ℃) of CeO_2[17], the first peak of CDC82 material shifts to higher temperature, indicating that the reduction of surface sites is weakened; and the second peak shifts to lower temperature. An opposite conclusion can be drawn that the reduction of bulk sites is highly enhanced. But, the two peaks of CDC82 material are lower than those of $Ce_{1-x}Zr_xO_{2-\delta}$[18−19], indicating that the catalytic property of CDC82 material is excellent.

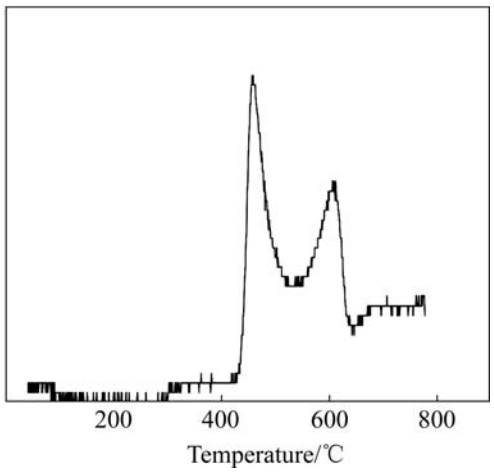

Fig.9 H_2-TPR profile of CDC82 material

Fig.10 shows the products and their contents of the catalytic reactions of CeO_2-methane and CDC82-methane at 850 ℃. Compared with the reaction between CeO_2 and methane, more CO and CO_2 and less H_2 exist in the reaction of CDC82 and methane when the mass of CeO_2 and CDC82 are the same. This indicates that Ce^{4+} ions are reduced more easily when they are partly replaced by Ca^{2+}. XRD results show that the CDC82 material remains in the fluorite structure and there is no evidence of formation of carbonaceous deposition after catalytic test.

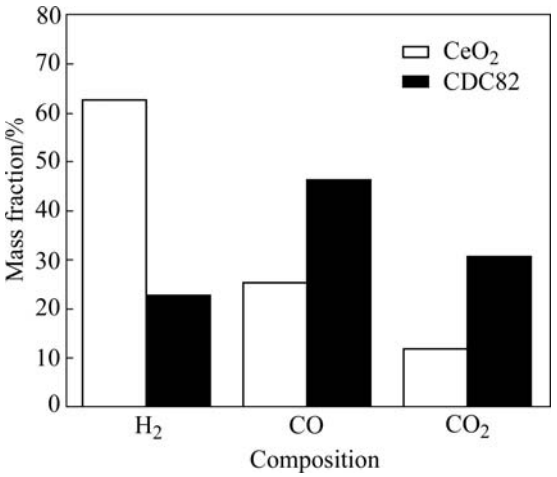

Fig.10 Composition and their contents of catalytic reactions of CeO_2 and CDC82 materials for CH_4

4 Conclusions

1) Thermal analysis (TG-DSC) shows that CDC82 material with fluorite structure forms and the mass decreases quickly from 567 ℃. There is an apparent exothermal peak at 829 ℃, but the TG curve becomes smooth after this temperature, indicating a possible transition of the crystal structure at 829 ℃. After the precursor is sintered at 750 ℃ for 4 h, CDC82 material with pure-fluorite structure is obtained.

2) The total conductivity is low and changes little with temperature increasing in air. It becomes higher wholly and increases more quickly with temperature increasing when the atmosphere changes from air to hydrogen. The total conductivity is 1.09 S/cm at 850 ℃. CDC82 and LSGM materials have bad chemical compatibility**.**

3) The catalytic property and bulk sites of CDC82 material are greatly enhanced when Ce^{4+} is partly replaced by Ca^{2+}. The most products are CO and H_2 in the catalytic reaction of CDC82 material for methane at 850 ℃. At the same time, a quantity of CO_2 emerges due to the strong oxidized property of CDC82 material.

References

[1] GORTE R J, VOHS J M. Novel SOFC anodes for the direct electrochemical oxidation of hydrocarbons [J]. Journal of Catalysis, 2003, 216: 477−486.

[2] HUANG Xian-liang, ZHAO Hai-lei, WU Wei-jiang, QIU Wei-hua. Recent process of anode materials for solid oxide fuel cells [J]. Journal of the Chinese Ceramic Society, 2005, 23(11): 1407−1413. (in Chinese)

[3] MINH N Q. Ceramic fuel cells [J]. J Am Ceram Soc, 1993, 76: 563−588.

[4] KOH J H, YOO Y S, PARK J W, LIM H C. Carbon deposition and cell performance of Ni-YSZ anode support SOFC with methane fuel [J]. Solid State Ionics, 2002, 149: 157−166.

[5] ZHA Shao-wu, GU Yun-feng, FU Qing-xi, XIA Chang-rong, PENG Ding-kun, MENG Guang-yao. Electrical properties of CeO_2-Y_2O_3 electrolyte SOFCs [J]. Journal of Functional Materials, 2000, 31(6): 612−614. (in Chinse)

[6] XIA Chang-rong, LIU Mei-lin. Low-temperature SOFCs based on $Gd_{0.1}Ce_{0.9}O_{1.95}$ fabricated by dry pressing [J]. Solid State Ionics, 2001, 144(3/4): 249−255.

[7] MATSUI T, INABA M, MINESSHIGE A, OGUMI Z. Electrochemical properties of ceria-based oxides for use in intermediate-temperature SOFCs [J]. Solid State Ionics, 2005, 176: 647−654.

[8] MOGENSEN M, SAMMES N M, TOMPSETT G A. Physical, chemical and electrochemical properties of pure and doped ceria [J]. Solid State Ionics, 2000, 129: 63−94.

[9] REN Yin-zhe, GUO Cong-feng, PENG Cheng, ZHANG Xiu-ying, LI Wu-ju, JIANG Kai. Conduction of rare earth complex oxides and their applications [J]. Chemical Research, 2001, 12(1): 59−64. (in Chinese)

[10] WANG Jian, SUN Jie, QIU Xin-ping, WU Zeng-hua, CHEN Li-quan. Hydrogen production from steam reforming of ethanol using Ni/CeO_2 and $Ni-Cu/CeO_2$ catalysts [J]. Chinese Journal of Power Source, 2006, 30(3): 234−237. (in Chinese)

[11] LI Chun-lin, FU Yi-lu, BIAN Guo-zhu . Performance of Ni/ZrO_2-CeO_2-$A1_2O_3$ catalyst prepared by different methods for carbon dioxide reforming of methane [J]. Chinese Journal of Catalysis, 2003, 24(3): 187−192. (in Chinese)

[12] XIN Jia-yu, WANG Hua, HE Fang, ZHANG Zhi-min. Thermodynamic and equilibrium composition analysis of using iron oxide as oxygen carrier in nonflame combustion technology [J]. Journal of Natural Gas Chemistry, 2005, 14: 248−253.

[13] LI Wen-bing, YUAN Zhang-fu, LIU Jian-xun, XU Cong, WEI Qing-song. Thermodynamics on the carbochlorination of titanium-bearing ores [J]. The Chinese Journal Process Engineering, 2004, 4(2): 121−123. (in Chinese)

[14] NING Xian-jin, LI Cheng-xin, LI Chang-jiu, YANG Guan-jun. Effect of powder structure on microstructure and electrical properties of plasma-sprayed 4.5mol% YSZ coating [J]. Vacuum, 2006, 80: 1261−1265.

[15] KOEP E, JIN Chun-ming, HALUSKA M, DAS R, ARAYAN R, SANDHAGE K, SNYDER R, LIU Mei-lin. Microstructure and electrochemical properties of cathode materials for SOFCs prepared via pulsed laser deposition [J]. Journal of Power Sources, 2006, 161: 250−255.

[16] BI Zhong-he, CHENG Mo-jie, DONG Yong-lai, WU He-jin, SHE Yun-chuan, YI Bao-lian. Electrochemical evaluation of $La_{0.6}Sr_{0.4}CoO_3$-$La_{0.45}Ce_{0.55}O_2$ composite cathode for anode-supported $La_{0.45}Ce_{0.55}O_2$-$La_{0.9}Sr_{0.1}Ga_{0.8}Mg_{0.2}O_{2.85}$ bilayer electrolyte solid oxide fuel cell [J]. Solid State Ionics, 2005, 176: 655−661.

[17] LARRONDO S, VIDAL M A, IRIGOYEN B , CRAIEVICH A F, LAMAS D G, FáBREGAS I O, LASCALEA G E, RECA N E W, AMADEO N. Preparation and characterization of Ce/Zr mixed oixdes and their use as catalysts for the direct oxidation of dry CH_4 [J]. Catalysis Today, 2005, 107/108: 53−59.

[18] LIN Rui, INMACULADA R R, BELIN B B, ANTONIO G R, SUN Gong-quan, XIN Qin. Catalytic activity and characterization of oxygen mobility on $Pt/Ce_{0.75}Zr_{0.25}O_2$ catalyst by isotopic exchange with ^{18}O [J]. Chinese Journal of Catalysis, 2006, 27(2): 109−114. (in Chinese)

[19] YE Qing, XU Bo-qing. Redox property of $Ce_{1-x}Zr_xO_2$ and its effect on CO_2 reforming of CH_4 [J]. Chinese Journal of Catalysis, 2006, 27(2): 151−156. (in Chinese)

(Edited by CHEN Wei-ping)